Mobile Robot Localization Using Robust Extended H_∞ Filtering

Fuwen Yang, Zidong Wang, Stanislao Lauria, and Xiaohui Liu

Abstract

In this paper, a novel methodology is provided for accurate localisation of mobile robot for an autonomous navigation based internal sensors and external sensors. A new robust extended H_∞ filter is developed to deal with nonlinear kinematic model of the robot and nonlinear distance measurements, together with process and measurement noises. The proposed filter relies on a two-step prediction-correction structure, which is similar to Kalman filter. Simulations are provided to demonstrate the effectiveness of the proposed method.

Keywords

Autonomous mobile robot; localisation; robust extended H_∞ filtering; navigation.

I. Introduction

Localisation is one of the fundamental problems for autonomous navigation of mobile robots. The knowledge about the position and orientation of a robot is useful in different tasks, such as office delivery, obstacle avoidance, for example. In the past, a variety of approaches for mobile robot localisation has been developed. They mainly differ in the techniques used to represent the belief of the robot about its current position, and according to the type of sensor information that is used for localisation. For the robot to be really autonomous, only on-board sensors must be used to perform localisation. This prevents it from using direct configuration measurements, and calls for suitable numerical processing of the data provided by the sensor equipment. The on-board sensors allow two different kinds of localisation: relative and absolute. The former is realized through the data provided by sensors measuring the dynamics of variables internal to the vehicle. One of the common methods used to estimate the current position is dead reckoning using internal sensors [3], [13], such as optical incremental encoders, which are fixed to the axis of the driving wheels or to the steering axis of the vehicle. At each sampling instant the position is estimated on the basis of the encoder increments along the sampling interval. A drawback of this method is that the errors of each measure are cumulative. The error in dead reckoning increases as the robot travels. This heavily degrades the position and orientation estimates of the vehicle, especially for long and winding trajectories [19].

Absolute localisation is performed processing the data provided by a proper set of sensors measuring some parameters of the environment in which the vehicle is operating. External sensors device, such as laser scanner,sonar, is generally used for this purpose. They are fixed to the vehicle and measure the distance with

This work was supported in part by the Engineering and Physical Sciences Research Council (EPSRC) of the U.K. under Grant GR/S27658/01, the Nuffield Foundation of the U.K. under Grant NAL/00630/G, and the Alexander von Humboldt Foundation of Germany.

F. Yang, Z. Wang, S. Lauria, and X. Liu are with the Department of Information Systems and Computing, Brunel University, Uxbridge, Middlesex, UB8 3PH, United Kingdom.

All correspondences concerning this paper should be addressed to Z. Wang. (Email: Zidong.Wang@brunel.ac.uk)

respect to parts of the known environment [2], [13]. They are also widely utilized for the guidance of autonomous vehicles with obstacle avoidance in unknown environment [8], [18]. The main drawback of absolute measures is their dependence on the characteristics of the environment. Possible changes to environmental parameters may give rise to erroneous interpretation of the measurements provided by the localisation algorithm.

In order to obtain the accurate localisation for mobile robot, an efficient method is to fuse together relative and absolute measurements using sensors of different nature. For this purpose, the localisation problem has been extensively studied in the robotics literature (see for instance [4], [12], [10], [11], [15], and the references therein). The mainstream approach for robot localisation is Bayesian estimation, which is based on stochastic assumptions about the process and measurement errors, and is aimed to constructing the posterior density of the current robot state, conditioned on all available measurements. In particular, when the process and measurement error processes are assumed Gaussian, the Bayesian approach results in the classical extended Kalman filtering (EKF) framework (see [1], [7], [14]). However, in robotics applications, the distribution of the sensor and process noise is generally multimodal and imprecisely known, and the nonlinearities of the system may seriously degrade the EKF performance. These limitations have been recognized in the literature, and several schemes have been proposed to overcome them. Notably, an adaptive EKF approach for on-line estimation of the noise statistics have been proposed in [10], [11]and [16], and joint Bayesian hypothesis testing and Kalman filtering have been proposed in [17]. A probabilistic confidence set approach has been presented in [15], which is optimal over a certain class of noise distributions. A Monte Carlo approach, where the noise density is represented by means of a set of randomly drawn samples, is proposed in [5]. The key idea of particle filter based method is to approximate the densities through samples (particles) according to the posterior distribution over robot poses [5]. The particle representation therefore, can provide universal density approximators without the assumption of Gaussian distribution and can adapt to the available computational resources by controlling the number of samples. Markov Chain Monte Carlo based method provides a posterior distribution estimation over robot poses [20]. The piecewise constant functions instead of Gaussians are used to approximate the distribution. However, the computation of piecewise constant representation is very demanding.

In this paper, an alterative to an adaptive EKF approach is proposed which is called as robust extended H_∞ filtering method that combines the data provided by internal sensors and external sensors together for estimates of robot position. The advantage of the robust extended H_∞ filtering techniques can consider the nonlinear system with unknown process noises and measurement noises. It is suitably used to the kinematic model of the robot and the knowledge of measure equipment. The techniques proposed here is superior to the extended Kalman filter (EKF) techniques proposed in the literature[6], for the estimation of robot localisation by considering the linearisation error and non-Gaussian noises in process and measurement. The main novelty of the robust extended H_∞ filtering here proposed is its capability of tolerably estimating robot localisation in unknown environment. The computation of the robust extended H_∞ filtering method is similar to the EKF. It can be implemented online.

The remainder of this paper is organized as follows. In Section II, the kinematics of the mobile robot is described and the scheme of absolute measurements are provided. A novel robust extended H_∞ filtering algorithm is developed in Section III for handling nonlinear process and measurement, and unknown noises. In Section IV a numerical simulation is provided to demonstrate the effectiveness of our algorithm. Some concluding remarks are provided in Section V.

Notation. The notation $X \geq Y$ (respectively, $X > Y$) where X and Y are symmetric matrices, means that $X - Y$ is positive semi-definite (respectively, positive definite). The superscript T stands for matrix transposition. By $\|f_k\|_R^2$, we denote the product $f_k^T R f_k$. We denote that Gramian matrix $R_x =< x, x >$, where $< x, x >$ stands for the inner product of x, i.e., $< x, x >= xx^T$, and x is a vector.

II. Kinematics of the Mobile Robot and the Absolute Measurement

Consider an unicycle-like mobile robot with two driving wheels, mounted on the left and right sides of the robot, with their common axis passing through the center of the robot (see Fig. 1). Localization of this

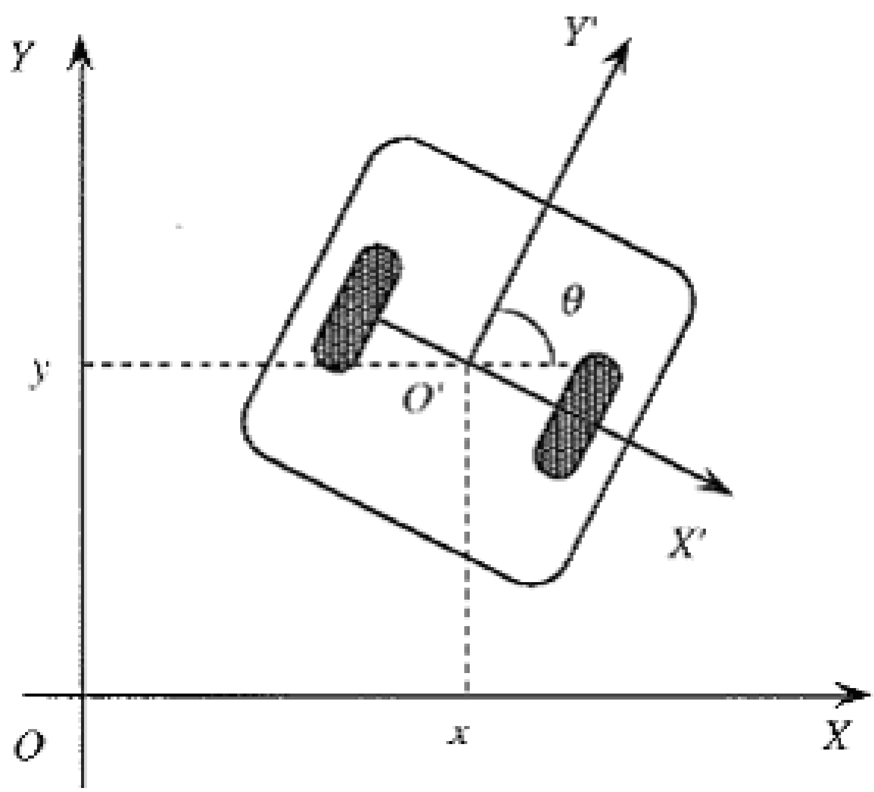

Fig. 1.

mobile robot in a two-dimensional space requires knowledge of the coordinates of the midpoint between the two driving wheels and of the angle between the main axis of the robot and the direction. The kinematic model of the unicycle robot is described by the following equations:

$$\begin{cases} \dot{x}(t) = v(t)\cos\theta(t) \\ \dot{y}(t) = v(t)\sin\theta(t) \\ \dot{\theta}(t) = \omega(t) \end{cases} \tag{1}$$

where

$$v(t) = \frac{v_R(t) + v_L(t)}{2} \tag{2}$$

$$\omega(t) = \frac{v_R(t) - v_L(t)}{d} \tag{3}$$

where $x(t)$ and $y(t)$ are the coordinates of the main axis midpoint between the two driving wheels, $\theta(t)$ is the angle between the robot forward axis and the x-direction, $v(t)$ and $\omega(t)$ are, respectively, the displacement and angular velocities of the robot, $v_R(t)$ and v_L are, respectively, the right and left displacement velocities of the robot, and d is the distance between the two wheels of robot. The encoders placed on the driving wheels provide a measure of the incremental angles over a sampling period. The odometric measures are used to obtain an estimate of the displacement and angular velocities, respectively, which are assumed to be constant over the sampling period. If we assume zero-order hold on $v(t)$ and $\omega(t)$, then the above system is discretized with sample time and expressed in linear form as

$$\begin{cases} x_{k+1} = x_k + \triangle T v_k \cos\theta_k \\ y_{k+1} = y_k + \triangle T v_k \sin\theta_k \\ \theta_{k+1} = \theta_k + \triangle T \omega_k \end{cases} \tag{4}$$

Let

$$z_k = \begin{bmatrix} x_k \\ y_k \\ \theta_k \end{bmatrix} \tag{5}$$

and

$$u_k = \begin{bmatrix} \triangle T v_k \\ \triangle T \omega_k \end{bmatrix} := \begin{bmatrix} u_{1,k} \\ u_{2,k} \end{bmatrix} \tag{6}$$

we rewrite (4) as:

$$z_{k+1} = f(z_k, u_k) \tag{7}$$

where

$$f(z_k, u_k) = z_k + \begin{bmatrix} u_{1,k}\cos\theta_k \\ u_{1,k}\sin\theta_k \\ u_{2,k} \end{bmatrix} \tag{8}$$

The distance and angle to the marker M are treated as the measurements (see Fig. 2). The azimuth ψ with respect to the x-axis and the distance from the robot's planar Cartesian coordinates (x, y) to the marker (x_M, y_m) at a time instant k can be related to the current system state variables x_k, y_k, and θ_k as follows:

$$d_k = \sqrt{(x_m - x_k)^2 + (y_m - y_k)^2} \tag{9}$$

$$\psi_k = \theta_k - \arctan(\frac{y_m - y_k}{x_m - x_k}) \tag{10}$$

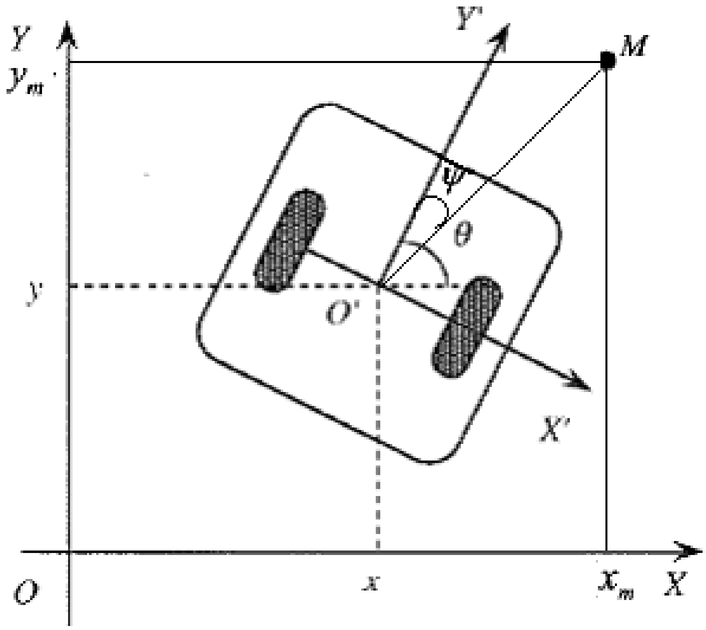

Fig. 2.

Let

$$m_k = \begin{bmatrix} d_k \\ \psi_k \end{bmatrix} \tag{11}$$

we rewrite (4) as:

$$m_k = g(z_k) \tag{12}$$

where

$$g(z_k) = \begin{bmatrix} \sqrt{(x_m - x_k)^2 + (y_m - y_k)^2} \\ \theta_k - \arctan(\frac{y_m - y_k}{x_m - x_k}) \end{bmatrix} \tag{13}$$

To this end, we obtain the system state equation and measurement equation for mobile robot navigation as follows:

$$z_{k+1} = f(z_k, u_k) \tag{14}$$
$$m_k = g(z_k) \tag{15}$$

III. A Robust Extended H_∞ Filter Design

Since $f(z_k, u_k)$ and $g(z_k)$ are nonlinear, we expand the nonlinear functions $f(z_k, u_k)$ and $g(z_k)$ in a Taylor series about the filtered estimates $\hat{z}_k$ as

$$\begin{aligned} f(z_k, u_k) &= f(\hat{z}_k, u_k) + A_k(z_k - \hat{z}_k) + \sigma_1 && (16)\\ g(z_k) &= g(\hat{z}_k) + C_k(z_k - \hat{z}_k) + \sigma_2 && (17) \end{aligned}$$

where

$$A_k = \begin{bmatrix} \frac{\partial f_x}{\partial x_k} & \frac{\partial f_x}{\partial y_k} & \frac{\partial f_x}{\partial \theta_k} \\ \frac{\partial f_y}{\partial x_k} & \frac{\partial f_y}{\partial y_k} & \frac{\partial f_y}{\partial \theta_k} \\ \frac{\partial f_\theta}{\partial x_k} & \frac{\partial f_\theta}{\partial y_k} & \frac{\partial f_\theta}{\partial \theta_k} \end{bmatrix}\Bigg|_{z_k=\hat{z}_k} = \begin{bmatrix} 1 & 0 & u_{1,k}\sin\theta_k \\ 0 & 1 & u_{1,k}\cos\theta_k \\ 0 & 0 & 1 \end{bmatrix}\Bigg|_{z_k=\hat{z}_k} \tag{18}$$

$$C_k = \begin{bmatrix} \frac{\partial g_d}{\partial x_k} & \frac{\partial g_d}{\partial y_k} & \frac{\partial g_d}{\partial \theta_k} \\ \frac{\partial g_\psi}{\partial x_k} & \frac{\partial g_\psi}{\partial y_k} & \frac{\partial g_\psi}{\partial \theta_k} \end{bmatrix}\Bigg|_{z_k=\hat{z}_k} = \begin{bmatrix} -\frac{(x_m - x_k)}{\sqrt{(x_m-x_k)^2+(y_m-y_k)^2}} & -\frac{(y_m - y_k)}{\sqrt{(x_m-x_k)^2+(y_m-y_k)^2}} & 0 \\ \frac{(y_m - y_k)}{(x_m-x_k)^2+(y_m-y_k)^2} & -\frac{(x_m - x_k)}{(x_m-x_k)^2+(y_m-y_k)^2} & -1 \end{bmatrix}\Bigg|_{z_k=\hat{z}_k} \tag{19}$$

and σ_1 and σ_2 represent the higher order terms of the Taylor series expansions.

Therefore, (11)-(12) can be written as:

$$\begin{aligned} z_{k+1} &= A_k z_k + w_k && (20)\\ m_k &= C_k z_k + v_k && (21) \end{aligned}$$

where

$$\begin{aligned} w_k &= f(\hat{z}_k, u_k) - A_k\hat{z}_k + \sigma_1 && (22)\\ v_k &= g(\hat{z}_k) - C_k\hat{z}_k + \sigma_2 && (23) \end{aligned}$$

A typical approach applied to the linearized model (20)-(21) is the extended Kalman filtering, where the nonlinear errors w_k and v_k are considered as Gaussian white noises. However, in mobile robot navigation, these assumptions are unpractical. They may seriously degrade the navigation accuracy (the extended Kalman filtering performance). Therefore, our objective of this paper is to find a robust filter for the system (20)-(21) such that the filtering error system satisfies H_∞ robustness performance constraint without the assumptions of that the nonlinear errors w_k and v_k are Gaussian white noises. More specifically, we want to find a filter such that the filtering error system satisfies the following requirement:

$$\frac{\sum_{k=0}^{N}\|\tilde{z}_k\|^2}{\|z_0 - \hat{z}_{0|-1}\|^2_{P^{-1}_{0|-1}} + \sum_{k=0}^{N-1}\|w_k\|^2_{Q_k^{-1}} + \sum_{k=0}^{N}\|v_k\|^2_{R_k^{-1}}} < \gamma^2, \tag{24}$$

for all nonzero w_k and v_k, where $\gamma > 0$ is a prescribed scalar and $\tilde{z}_k = z_k - \hat{z}_k$.

The design problem stated above will be referred to as the robust extended H_∞ filtering problem.

Theorem 1: (**finite horizon extended H_∞ filter**) For a given scalar $\gamma > 0$, if the $\begin{bmatrix} A_k & B_k \end{bmatrix}$ has full rank, the there exists a filter which achieves the performance (24) if and only if the filtered error covariance matrix $P_{k|k}$ satisfies

$$P^{-1}_{k|k} = P^{-1}_{k|k-1} + C_k^T R_k^{-1} C_k - \gamma^{-2} I > 0, \quad 0 \le k \le N, \tag{25}$$

where the predicted error covariance matrix $P_{k|k-1}$ satisfies the Riccati recursion:

$$P_{k|k-1} = A_{k-1}P_{k-1|k-1}A_{k-1}^T + Q_{k-1}, \tag{26}$$

The filtered estimates $\hat{z}_{k|k}$ are recursively computed as

$$\hat{z}_{k|k} = \hat{z}_{k|k-1} + K_k(y_k - g(\hat{z}_k)) \tag{27}$$

where

$$K_k = P_{k|k-1}C_k^T(C_kP_{k|k-1}C_k^T + R_k)^{-1} \tag{28}$$

and the predicted estimates $\hat{z}_{k|k-1}$ are

$$\hat{z}_{k|k-1} = f(\hat{z}_k, u_k) \tag{29}$$

Proof: The proof of Theorem 1 is presented in the appendix. ■

IV. Simulation Results

In order to demonstrate the advantages of our proposed filter, we compare the performances of the robust extended H_∞ filter with the traditional extended Kalman filter. The filters are used to estimate the mobile robot state (position and orientation in planar motion) by the odometry and the information from the absolute marker detection. The algorithms are run on the simulated data. For comparison purposes, we have performed numerical simulations in three different situations.

In the first simulation, the process and measurement errors w_k and v_k are assumed to be Gaussian random sequences. The process error covariance matrix is chosen to be diagonal and time-invariant. The standard deviation of the system position for x and y coordinates is taken to be $e_x = e_y = 0.01m$ (variances $\delta_x^2 = \delta_y^2 = 10^{-4}m^2$, and the orientation standard deviation $e_\theta = 0.5^o$ (variance $\delta_\theta^2 = 7.62 \cdot 10^{-4}\text{rad}^2$). The measurement error covariance matrix is also chosen to be diagonal and time-invariant. The measurement standard deviation for the distance to the absolute marker is taken to be $e_d = 0.01m$ (variances $\delta_d^2 = 10^{-4}m^2$, and the azimuth standard deviation $e_\theta = 0.5^o$ (variance $\delta_\theta^2 = 7.62 \cdot 10^{-4}\text{rad}^2$). The simulation results are depicted in Figs. 3-6. Fig. 3 and Fig. 4 show the robot position and its estimate, and the robot angle and its estimate, respectively, using the EKF algorithm. Fig. 5 and Fig. 6 show the robot position and its estimate, and the robot angle and its estimate, respectively, using the robust extended H_∞ filter. It is seen from the simulation results that the robust extended H_∞ filter is not better than the EKF. This is not surprising since its Gaussian noise hypotheses are exactly satisfied. The maximum distance between the actual trajectory and its estimate is 0.0228 by using the EKF and 0.0244 using the robust extended H_∞ filter. The maximum angle error between the actual angle and its estimate is 0.4075 by using the EKF and 0.3930 using the robust extended H_∞ filter.

In the second simulation, the process and measurement errors w_k and v_k have been generated as sinusoid disturbance signals. The process error signals are chosen to be diagonal and time-varying sinusoid $sin(100t)$, all of which amplitudes are 0.002. The measurement error signals are chosen to be diagonal and time-varying sinusoid as $sin(100t)$, for all of which the amplitudes are 0.001. The simulation results are depicted in Figs. 7-10. Fig. 7 and Fig. 8 show the robot position and its estimate, and the robot angle and its estimate, respectively, using the EKF algorithm. Fig. 9 and Fig. 10 show the robot position and its estimate, and the robot angle and its estimate, respectively, using the robust extended H_∞ filter. It is seen from the simulation results that the robust extended H_∞ filter yields much better performance than the EKF. The maximum distance between the actual trajectory and its estimate is 0.0391 by using the EKF and 0.0257 using the robust extended H_∞ filter. The maximum angle error between the actual angle and its estimate is 0.4594 by using the EKF and 0.4467 using the robust extended H_∞ filter.

In the third simulation, the process and measurement errors w_k and v_k are assumed as outlier disturbances. The outliers occur at the 2nd second and 3rd second, each of which lasts for 0.05 second. The process error signals are chosen to be diagonal and outliers, for all of which the amplitudes are 0.5. Also, the measurement error signals are chosen to be diagonal and outliers, for all of which the amplitudes are 0.1. The simulation results are depicted in Figs. 11-14. Fig. 11 and Fig. 12 show the robot position and its estimate, and the robot angle and its estimate, respectively, using the EKF algorithm. Fig. 13 and Fig. 14 show the robot position and its estimate, and the robot angle and its estimate, respectively, using the robust extended H_∞ filter. It is seen from the simulation results that the robust extended H_∞ filter yields a better performance than the EKF. The maximum distance between the actual trajectory and its estimate is 0.0601 by using the EKF and 0.0548 using the robust extended H_∞ filter. The maximum angle error between the actual angle and its estimate is 1.0182 by using the EKF and 0.9689 using the robust extended H_∞ filter.

V. Conclusions

In this paper, we have provided a novel methodology for accurate localisation of mobile robot for an autonomous navigation based internal sensors and external sensors. A new robust extended H_∞ filter has been developed to deal with nonlinear kinematic model of the robot and nonlinear distance measurements, together with process and measurement noises. The proposed filter relies on a two-step prediction-correction structure, which is similar to Kalman filter. On the simulated experiments, the robust filter has provided superior performance with respect to the EKF approach for the practical situations, where the system is subject to polarization, misalignments, and offsets, that cannot be effectively modeled as Gaussian noise.

References

[1] B. D. O. Anderson and J. B. Moore, *Optimal Filtering.* Englewood Cliffs, NJ: Prentice-Hall, 1979.

[2] M. Betke and L. Gurvits, Mobile robot localization using landmarks, *IEEE Trans. Robot. Autom.*, vol. 13, no. 2, pp. 251263, Apr. 1997.

[3] J. Borenstein and L. Feng, Measurement and correction of systematic odometry errors in mobile robots, *IEEE Trans. Robot. Autom.*, vol. 12, no. 6, pp. 869-880, Dec. 1996.

[4] G. Calafiore, Reliable localization using set-valued nonlinear filters, *IEEE Trans. Systems, Man and Cybernetics-Part A*, vol. 35, no. 2, pp. 189-197, March 2005.

[5] F. Dellaert, D. Fox,W. Burgard and S. Thrun, Monte Carlo localization for mobile robots, in *Proc. IEEE Int. Conf. Robot. Autom.*, Detroit, MI, May 1999, pp. 1322-1328.

[6] G. A. Einicke and B. White, Robust extended Kalman filtering, *IEEE Trans. Signal Process.*, vol. 47, no. 9, pp. 2596-2599, Sep. 1999.

[7] E. Fabrizi, G. Oriolo, S. Panzieri and G. Ulivi, A KF-based localization algorithm for nonholonomic mobile robots, in *Proc. 6th IEEE Mediterranean Conf.*, Alghero, Italy, Jun. 1998, pp. 130-135.

[8] F. Figueroa and A. Mahajan, A robust navigation system for autonomous vehicles using ultrasonics, *Control Engineering Practice*, vol. 2, no. 1, pp. 49-59, 1994.

[9] B. Hassibi, A. H. Sayed, and T. Kailath, *Indefinite Quadratic Estimation and Control: A Unified Approach to* H_2 *and* H_∞ *Theories*, Philadelphia, PA: SIAM, 1999.

[10] L. Jetto, S. Longhi and G. Venturini, Development and experimental validation of an adaptive extended Kalman filter for the localization of mobile robots, *IEEE Trans. Robot. Autom.*, vol. 15, no. 2, pp. 219-229, Apr. 1999.

[11] L. Jetto, S. Longhi and D. Vitali, Localization of a wheeled mobile robot by sensor data fusion based on a fuzzy logic adaptive Kalman filter, *Control Engineering Practice*, vol. 7, no. 6, pp. 763-771, June 1999.

[12] M. Kieffer, L. Jaulin, E. Walter and D. Meizel, Robust autonomous robot localization using interval analysis, *Reliable Comput.*, vol. 6, no. 3, pp. 337-362, 2000.

[13] E. Kiriy and M. Buehler, Three-state Extended Kalman Filter for Mobile Robot Localization, *Technical Report*, McGill University, 2002.

[14] J. J. Leonard and H. F. Durrant-Whyte, *Directed Sonar Sensing for Mobile Robot Navigation*. Boston, MA: Kluwer, 1992.

[15] R. Mandelbaum and M. Mintz, A confidence set approach to mobile robot localization, in *Proc. IEEE/RSJ Int. Conf. Intell. Robots Syst.*, Osaka, Japan, 1996, pp. 481-488.

[16] Q. H. Meng, Y. C. Sun and Z. L. Cao, Adaptive extended Kalman filter (AEKF)-based mobile robot localization using sonar, *Robotica*, vol. 18, no. 5, pp. 459-473, 2000.

[17] S. I. Roumeliotis and G. A. Bekey,Bayesian estimation and Kalman filtering: a unified framework for mobile robot localization, in *Proc. IEEE Int. Conf. Robot Autom.*, San Francisco, CA, Apr. 2000, pp. 2985-2992.

[18] K. T. Sutherland and W. B. Thompson, Localizing in unstructured environments: dealing with the errors, *IEEE Trans. Robot. Autom.*, vol. 10, no. 6, pp. 740-754, Jun. 1994.

[19] C. M. Wang, Localization estimation and uncertainty analysis for mobile robots, in *Proc. Int. Conf. Robot. Automat.*, pp. 1230-1235, 1988.

[20] D. Fox, W. Burgard, and S. Thrun, Markov localization for mobile robots in dynamic environments, *Journal of Artificial Intelligence Research*, vol. 11, pp.391C427, 1999.

APPENDIX

The proof of Theorem 1.

Before the proof of Theorem 1, we provide the following lemma.

Lemma 1: (Krein space Kalman filter)[9](Given a Krein space discrete-time system:

$$x_{k+1} = A_k x_k + B_k w_k \tag{30}$$

$$y_k = C_k x_k + v_k \tag{31}$$

with the Gramian matrix

$$\langle \begin{bmatrix} x_0 \\ w_j \\ v_j \end{bmatrix}, \begin{bmatrix} x_0 \\ w_k \\ v_k \end{bmatrix} = \begin{bmatrix} P_{0|-1} & 0 & 0 \\ 0 & Q_k\delta_{jk} & 0 \\ 0 & 0 & R_k\delta_{jk} \end{bmatrix} \rangle \tag{32}$$

both of which can be obtained from Krein space mapping corresponding to the indefinite quadratic function:

$$J = \|x_0 - \hat{x}_{0|-1}\|^2_{P^{-1}_{0|-1}} + \sum_{k=0}^{N-1} \|w_k\|^2_{Q_k^{-1}} + \sum_{k=0}^{N} \|(y_k - C_k x_k)\|^2_{R_k^{-1}} \tag{33}$$

If $P_{0|-1} > 0$, $Q_k > 0$, R_k is invertible, and $\begin{bmatrix} A_k & B_k \end{bmatrix}$ has full rank for all k, the existence condition for the Krein space Kalman filter is given by:

$$P^{-1}_{k|k} = P^{-1}_{k|k-1} + C_k^T R_k^{-1} C_k > 0 \tag{34}$$

In addition, if this existence condition is satisfied, then the Krein space Kalman filtering equations is governed by: (Measurement update):

$$\hat{x}_{k|k} = \hat{x}_{k|k-1} + K_k(y_k - C_k\hat{x}_{k|k-1}) \tag{35}$$

$$P_{k|k} = P_{k|k-1} - P_{k|k-1}C_k^T(C_kP_{k|k-1}C_k^T + R_k)^{-1}C_kP_{k|k-1} \tag{36}$$

where the gain matrix K_k is defined by:

$$K_k = P_{k|k-1}C_k^T(C_kP_{k|k-1}C_k^T + R_k)^{-1} \tag{37}$$

(Time update):

$$\hat{x}_{k+1|k} = A_k\hat{x}_{k|k} \tag{38}$$

$$P_{k+1|k} = A_kP_{k|k}A_k^T + B_kQ_kB_k^T \tag{39}$$

and the minimum point of the indefinite quadratic function J is provided by:

$$\min J(x_0, w, y) = \sum_{k=0}^{N} \|e_k\|^2_{(C_kP_{k|k-1}C_k^T+R_k)^{-1}} \tag{40}$$

where the innovations e_k are defined by

$$e_k = y_k - \hat{y}_{k|k-1} = y_k - C_k\hat{x}_{k|k-1} \tag{41}$$

Proof: In order to apply the approach of Krein space kalman filtering to the robust H_∞ extended filtering problem, we will adopt a mapping from the Hilbert space to the Krein space to solve the deterministic minimisation problem. In Krein space, the minimisation problem of a quadratic function can be cast into the Krein space Kalman filtering problem. We now recast the H_∞ performance (24) into the form of (33). We define

$$\begin{aligned} J_\infty &= \|z_0 - \hat{z}_{0|-1}\|^2_{P_{0|-1}^{-1}} + \sum_{k=0}^{N-1}\|w_k\|^2_{Q_k^{-1}} + \sum_{k=0}^{N}\|v_k\|^2_{R_k^{-1}} - \gamma^{-2}\sum_{k=0}^{N}\|\tilde{z}_k\|^2 \\ &= \|z_0 - \hat{z}_{0|-1}\|^2_{P_{0|-1}^{-1}} + \sum_{k=0}^{N-1}\|w_k\|^2_{Q_k^{-1}} + \sum_{k=0}^{N}\|m_k - C_kz_k\|^2_{R_k^{-1}} - \gamma^{-2}\sum_{k=0}^{N}\|z_k - \hat{z}_{k|k}\|^2 \\ &= \|z_0 - \hat{z}_{0|-1}\|^2_{P_{0|-1}^{-1}} + \sum_{k=0}^{N-1}\|w_k\|^2_{Q_k^{-1}} + \sum_{k=0}^{N}\|\tilde{m}_k - \tilde{C}_kz_k\|^2_{\tilde{R}_k^{-1}} \end{aligned} \tag{42}$$

where

$$\tilde{m}_k = \begin{bmatrix} m_k \\ \hat{z}_{k|k} \end{bmatrix}, \quad \tilde{C}_k = \begin{bmatrix} C_k \\ I \end{bmatrix}, \quad \tilde{R}_k = \begin{bmatrix} R_k & 0 \\ 0 & -\gamma^2 I \end{bmatrix} \tag{43}$$

Then by Lemma 1, we can introduce the following Krein space system:

$$z_{k+1} = A_kz_k + w_k \tag{44}$$

$$\tilde{m}_k = \tilde{C}_kz_k + v_k \tag{45}$$

with the Gramian matrix

$$\langle \begin{bmatrix} z_0 \\ w_j \\ v_j \end{bmatrix}, \begin{bmatrix} z_0 \\ w_k \\ v_k \end{bmatrix} = \begin{bmatrix} P_{0|-1} & 0 & 0 \\ 0 & Q_k\delta_{jk} & 0 \\ 0 & 0 & \tilde{R}_k\delta_{jk} \end{bmatrix} \rangle \tag{46}$$

Now we are in a position to apply Lemma 1 to the robust H_∞ extended filtering problem. Note that there exist the following correspondences between the weighting matrices in the cost function (33) of Kalman filtering and that of H_∞ extended filtering in (43):

$$Q_k \longmapsto Q_k, \quad R_k \longmapsto \tilde{R}_k. \tag{47}$$

In addition to the following correspondences between the system matrices of Kalman filtering and and that of H_∞ extended filtering:

$$A_k \longmapsto A_k, \quad B_k \longmapsto I, \quad C_k \longmapsto \tilde{C}_k. \tag{48}$$

From the above correspondences, we can check that

$$\begin{aligned} P_{k|k}^{-1} &= P_{k|k-1}^{-1} + \tilde{C}_k^T \tilde{R}_k^{-1} \tilde{C}_k \\ &= P_{k|k-1}^{-1} + C_k^T R_k^{-1} C_k - \gamma^{-2} I \end{aligned} \tag{49}$$

which is identical to (25). On the other hand, we, by using Lemma 1, have

$$\begin{aligned} \hat{z}_{k|k} &= \hat{z}_{k|k-1} + P_{k|k-1}\tilde{C}_k^T (\tilde{C}_k P_{k|k-1} \tilde{C}_k^T + \tilde{R}_k)^{-1} (\tilde{m}_k - \tilde{C}_k \hat{z}_{k|k-1}) \\ &= \hat{z}_{k|k-1} + P_{k|k-1} \begin{bmatrix} C_k^T & I \end{bmatrix} \begin{bmatrix} I & -\hat{R}_k^{-1} C_k P_{k|k-1} \\ 0 & I \end{bmatrix} \\ &\quad \cdot \begin{bmatrix} \hat{R}_k & 0 \\ 0 & -\gamma^{-2} I + (P_{k|k-1}^{-1} + C_k^T C_k)^{-1} \end{bmatrix}^{-1} \begin{bmatrix} I & 0 \\ -P_{k|k-1} C_k^T \hat{R}_k^{-1} & I \end{bmatrix} \begin{bmatrix} m_k - C_k \hat{z}_{k|k-1} \\ \hat{z}_{k|k} - \hat{z}_{k|k-1} \end{bmatrix} \end{aligned} \tag{50}$$

where

$$\hat{R}_k = R_k + C_k P_{k|k-1} C_k^T \tag{51}$$

By tedious but direct matrix inverse manipulation, we get

$$\hat{z}_{k|k} = \hat{z}_{k|k-1} + P_{k|k-1} C_k^T \hat{R}_k^{-1} (m_k - C_k \hat{z}_{k|k-1}) \tag{52}$$

which is same as (27). This completes the proof. ■

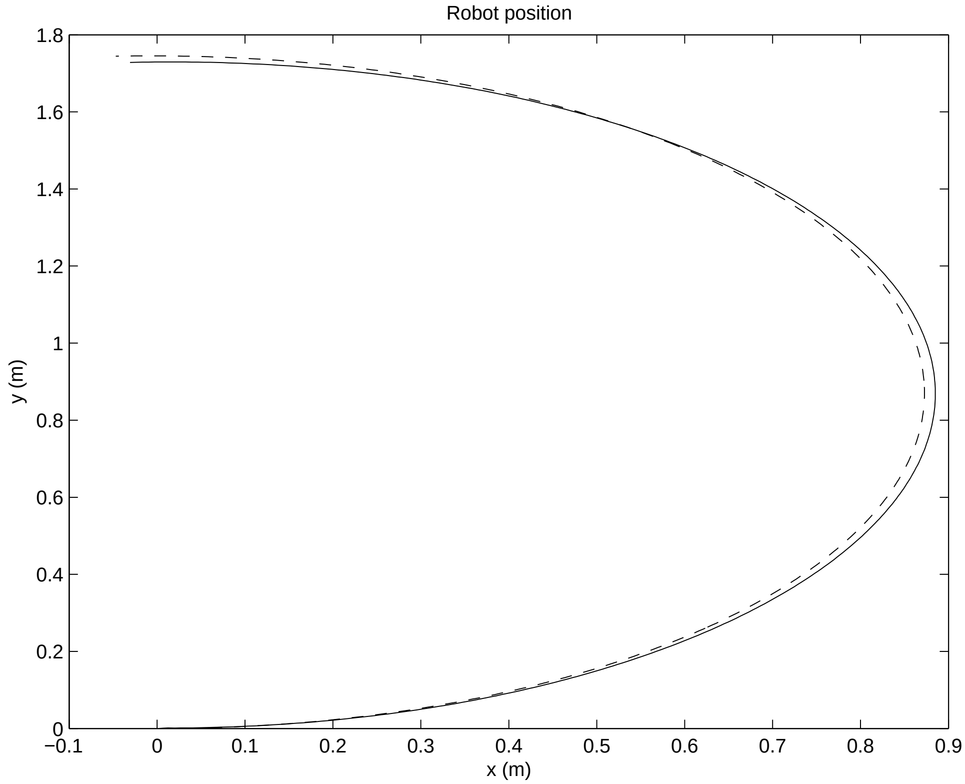

Fig. 3. Actual robot trajectory (dashed line) in the x-y plane and its estimate (solid line) by using EKF.

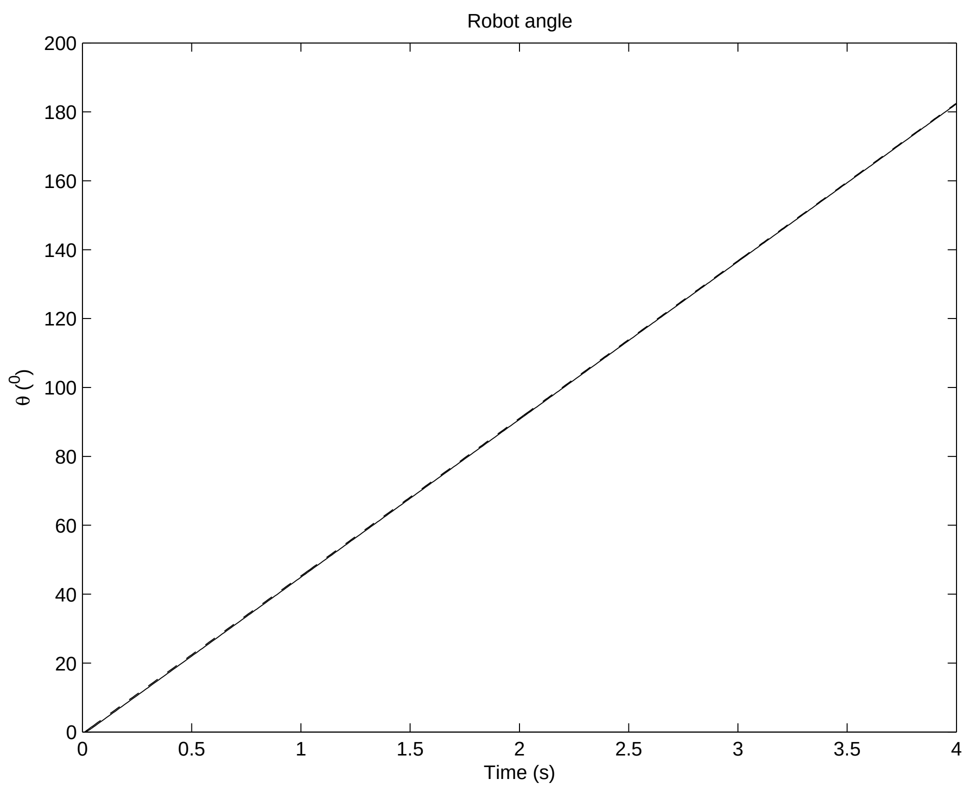

Fig. 4. Actual robot angle (dashed line) and its estimate (solid line) by using EKF.

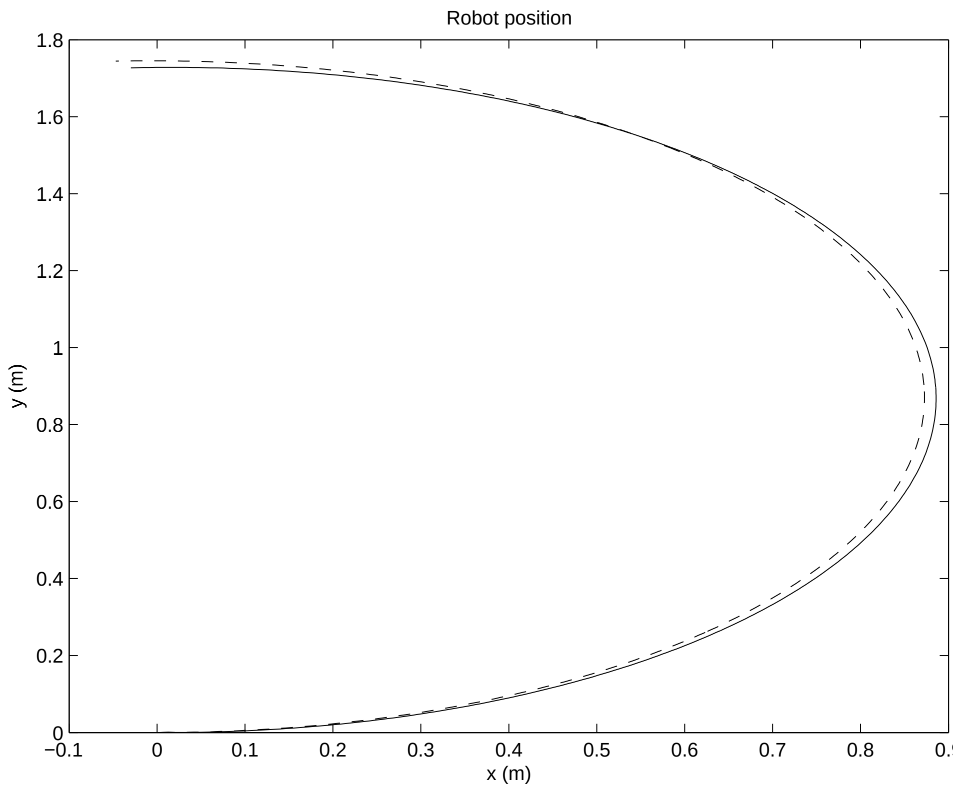

Fig. 5. Actual robot trajectory (dashed line) in the x-y plane and its estimate (solid line) by using our method.

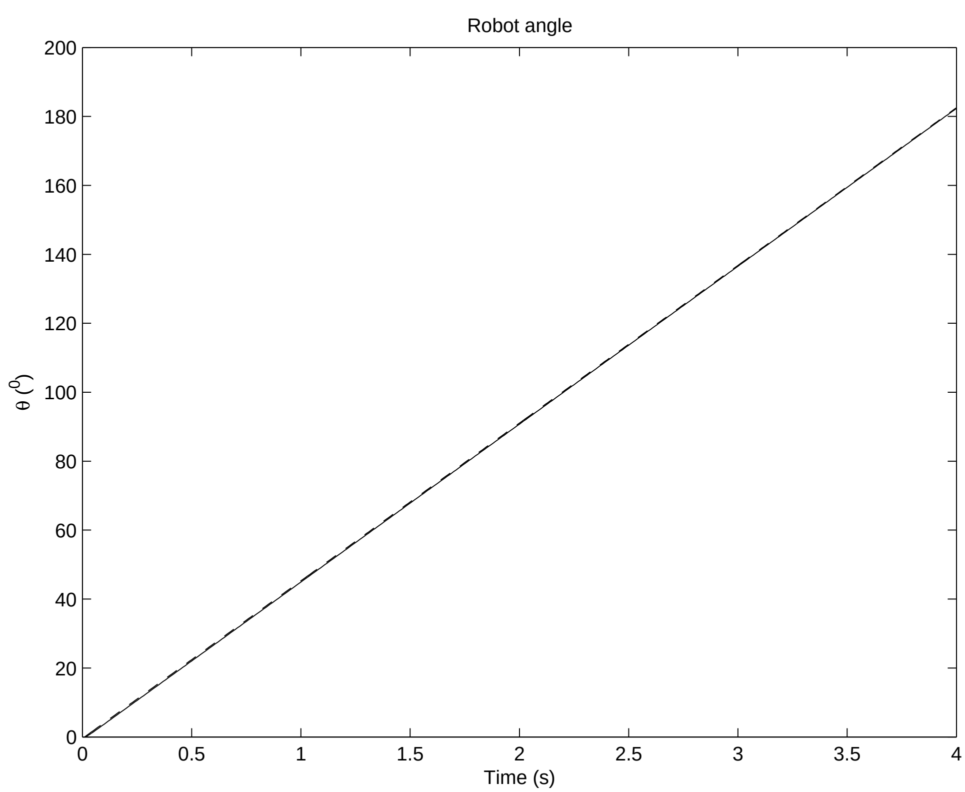

Fig. 6. Actual robot angle (dashed line) and its estimate (solid line) by using our method.

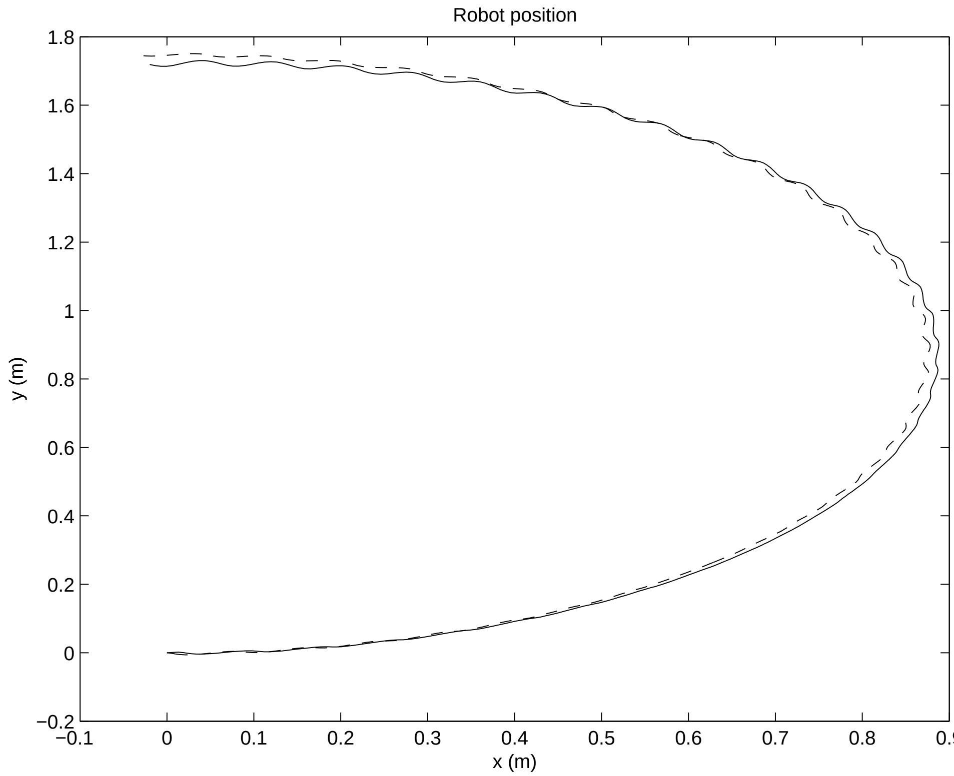

Fig. 7. Actual robot trajectory (dashed line) in the x-y plane and its estimate (solid line) by using EKF.

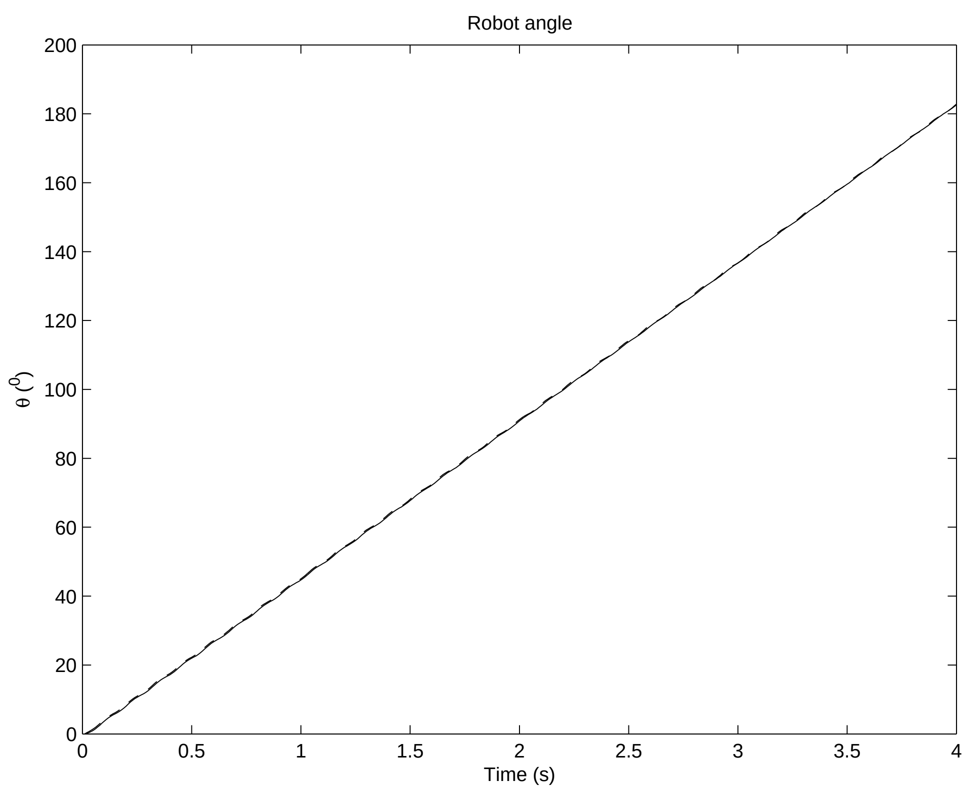

Fig. 8. Actual robot angle (dashed line) and its estimate (solid line) by using EKF.

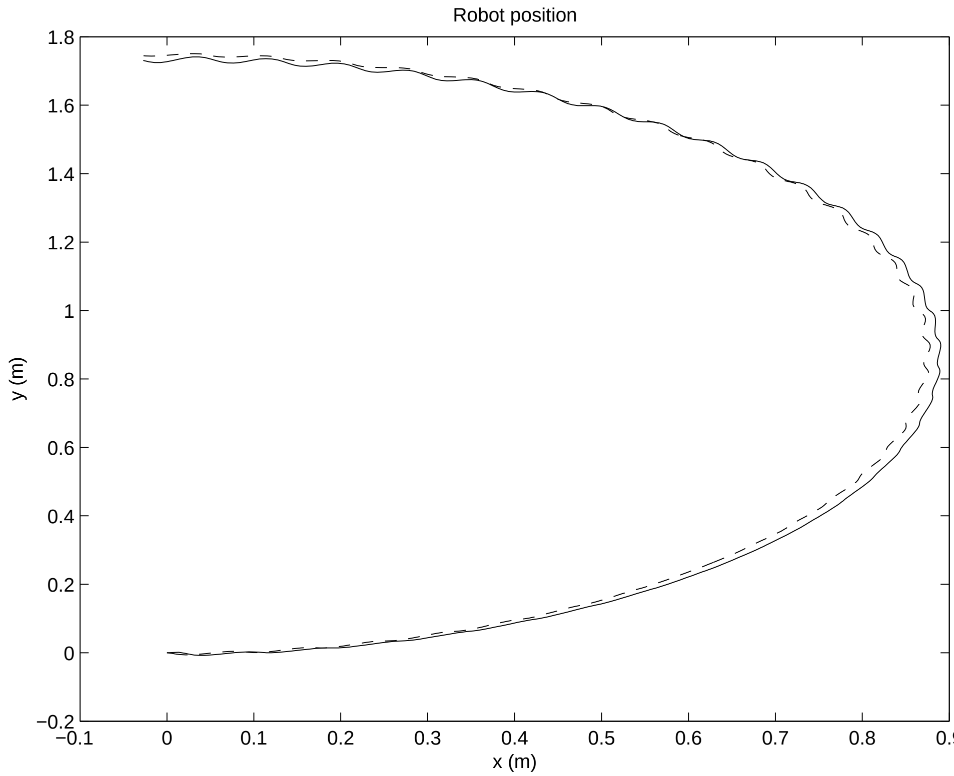

Fig. 9. Actual robot trajectory (dashed line) in the x-y plane and its estimate (solid line) by using our method.

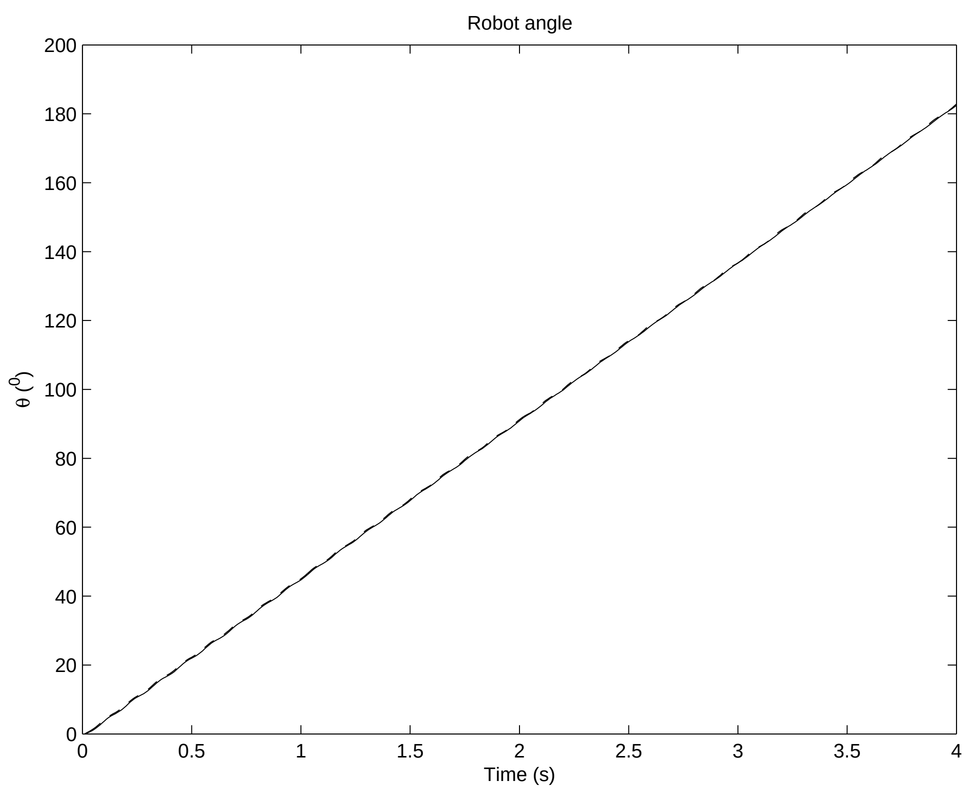

Fig. 10. Actual robot angle (dashed line) and its estimate (solid line) by using our method.

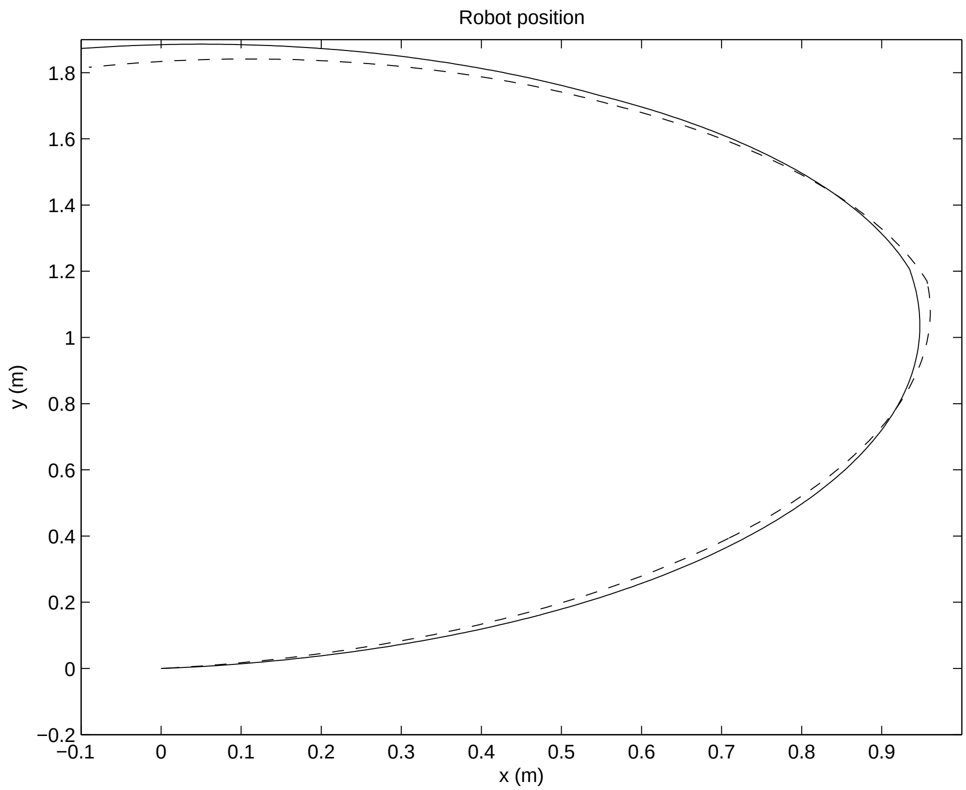

Fig. 11. Actual robot trajectory (dashed line) in the x-y plane and its estimate (solid line) by using EKF.

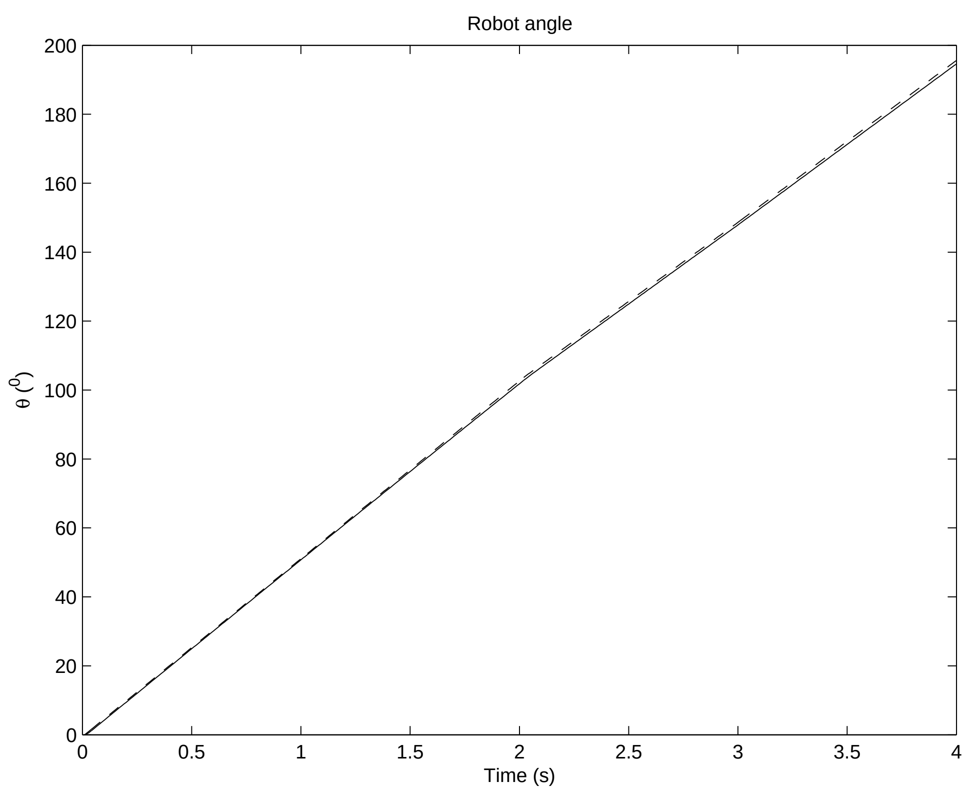

Fig. 12. Actual robot angle (dashed line) and its estimate (solid line) by using EKF.

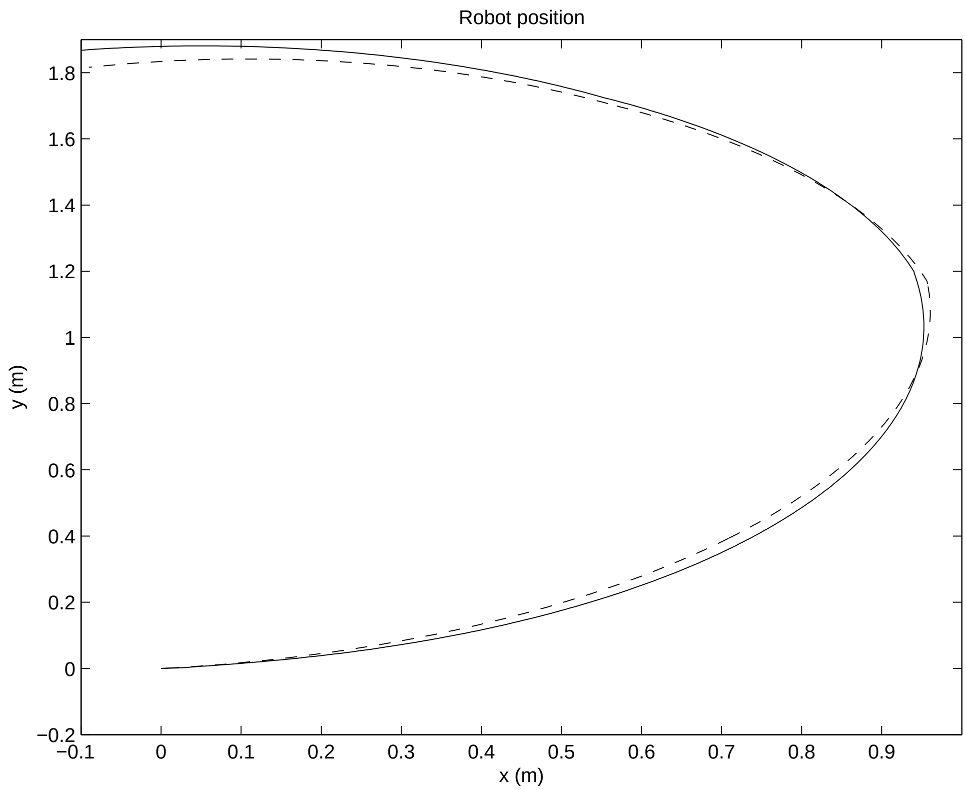

Fig. 13. Actual robot trajectory (dashed line) in the x-y plane and its estimate (solid line) by using our method.

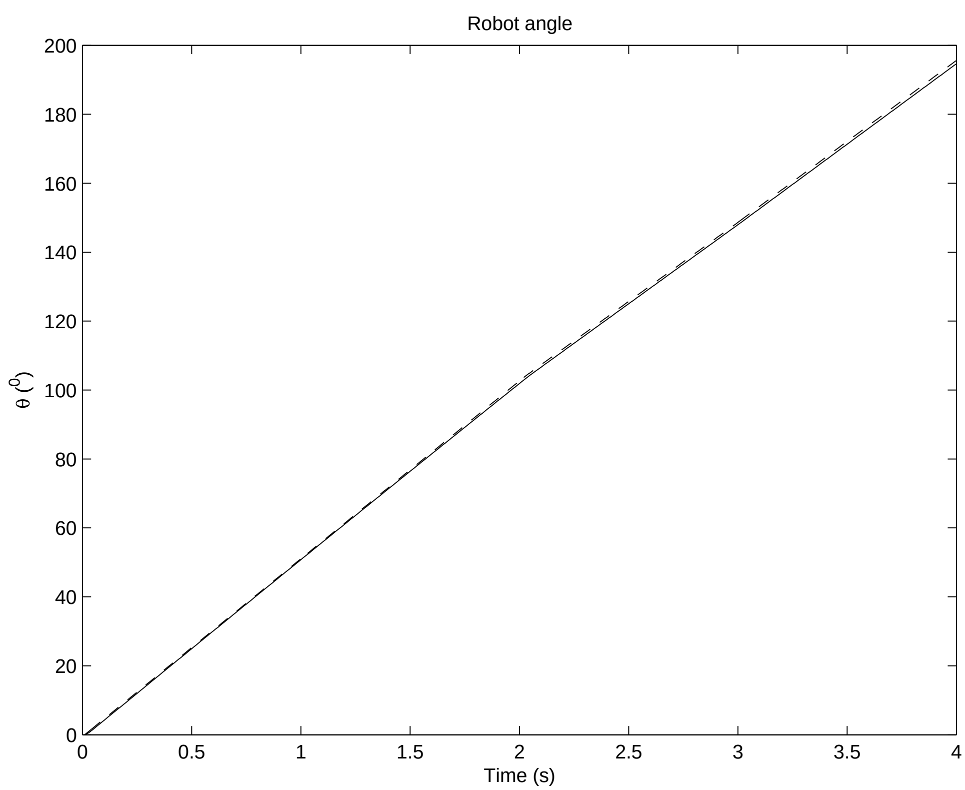

Fig. 14. Actual robot angle (dashed line) and its estimate (solid line) by using our method.